Desalination and Water Treatment
www.deswater.com
doi: 10.1080/19443994.2015.1061453

57 (2016) 12608–12619
June

Taylor & Francis
Taylor & Francis Group

Starch-functionalized magnetite nanoparticles for hexavalent chromium removal from aqueous solutions

P.N. Singh, D. Tiwary, I. Sinha*

Department of Chemistry, Indian Institute of Technology (Banaras Hindu University), Varanasi 221005, India, Tel./Fax: +91 542 6702876; emails: pnsingh.res.apc@itbhu.ac.in (P.N. Singh), dtiwari.apc@itbhu.ac.in (D. Tiwary), isinha.apc@itbhu.ac.in (I. Sinha)

Received 2 December 2014; Accepted 16 May 2015

ABSTRACT

Superparamagnetic starch-functionalized magnetite nanoparticles (SMNPs), ranging from 6 to14 nm, were prepared by a co-precipitation synthesis protocol. The SMNPs were used as nanoadsorbents for the removal of Cr(VI) from aqueous medium by the batch adsorption technique. The SMNPs adsorption capacity was found to decrease with the increase in the pH of the Cr(VI) solution. Under optimum pH conditions, the maximum experimental adsorption capacity of SMNPs for Cr(VI) was found to be 26.6 mg g^{-1}. While the adsorption was endothermic, the equilibrium adsorption data could be best fitted to the Freundlich adsorption isotherm model and its kinetics was in agreement with the pseudo-second-order rate equation. The SMNPs could be easily regenerated because of low adsorption activation energy. The SMNPs capacity for Cr(VI) removal remained almost undiminished even after its repeated use.

Keywords: Adsorption; Chromium; Starch; Magnetite nanoparticles; Magnetic separation

1. Introduction

Global industrialization has significantly increased the concentration of chromium in the environment and is at present one of the top toxic pollutants listed by US EPA. Chromium (Cr) is a frequent industrial effluent from different types of industries such as electroplating, metal finishing processes, tanning of leather, pigment, paints, dyes, and paper industries [1–4]. Among the two main oxidation states of Cr in aqueous medium, Cr (VI) is more toxic than Cr(III) [5–10]. The permissible concentration of Cr(VI) in drinking water is 0.05 ppm [11–13]. However, the US EPA survey reports that the concentration of Cr(VI) in different wastewaters range from 50 to 100 ppm. This is obviously much higher than the permitted level. Accordingly, a large number of conventional methods such as reduction, reverse osmosis, electrodialysis, ion exchange, and adsorption have been developed for the removal of Cr(VI) from aqueous medium. Among these, adsorption is an effective, efficient, and economic technique for wastewater treatment [14–19]. In this technique, depending on the nature of adsorbent–adsorbate interaction, there is a possibility of recovery and reuse of the adsorbent [20,21]. Magnetic nanoparticles are especially attractive since previous reports have shown them to be good adsorbents of heavy metal ions and are also easily separated using a suitable magnet [22].

*Corresponding author.

Ensuring better dispersion of nanoparticles in aqueous medium [23–25] is important for preserving their surface properties. For this purpose, presently non-toxic biocompatible stabilizers are preferred. Among various possibilities, the biodegradable water soluble and abundantly found starch is an attractive alternative. Starch is a branched, hydrophilic, and cross-linked long-chain polymer of D-glucose which may offer neutral-free hydroxyl functional groups with the possibility of binding to diverse chemical groups and ions, thus enhancing surface activity functionalized magnetic nanoparticles. This advantage when combined with the colloidal magnetic stability opens up large number of prospective applications such as drug delivery, gene delivery, magnetic resonance imaging, tissue engineering, enzyme immobilization, hyperthermia, and metal adsorption [26,27].

We demonstrate the formation of fine-sized superparamagnetic SMNPs as a new adsorbent for removal of Cr(VI) from aqueous medium. Such nanoparticles can easily be separated by magnetic decantation, then regenerated and redispersed in aqueous medium for reuse. The objectives of this study were therefore to (1) prepare superparamagnetic SMNPs and then utilize these nanoadsorbents for the removal of Cr(VI) from aqueous medium; (2) understand the mechanism of Cr (VI) adsorption onto the surface of nanoscale SMNPs; and (3) adsorbent recovery and recycling ability.

2. Experimental methods

2.1. Synthesis of SMNPs

Materials used in the synthesis of starch-functionalized magnetite nanoparticles were ferrous sulfate heptahydrate (Merck), NaOH (Merck), and starch. All chemicals used were of analytical grade and used without further purification. Ferrous sulfate heptahydrate (0.2 M) was dissolved in appropriate amount in distilled water and subjected to mechanical stirring for 15 min. To this 2 wt% of freshly prepared aqueous starch solution was added with continuous mechanical stirring for another 15 min to obtain a mixed solution. Now this solution was added drop wise into a previously heated 0.4 M NaOH solution such that the overall reaction mixture temperature was always maintained at 80°C. After completing the addition, the whole reaction mixture was heated at 80°C for two more hours until dark black precipitate formation was observed. The pH of the reaction mixture was above 8. Now the precipitate obtained was separated by magnetic decantation. The precipitate was then repeatedly washed with distilled water in order to remove excess NaOH and finally washed with absolute alcohol until the washings became neutral. Thereafter, the precipitate was dried at 40°C in a hot air oven. The dried powder samples were ground in an agate mortar and used further for material characterization and adsorption studies [28–30].

2.2. Adsorption experiments

The stock solution of Cr(VI) ions was prepared by dissolving a known amount of potassium dichromate in distilled water. Then the pH of the solution was adjusted by adding required amounts of 0.1 M HNO_3 or 0.1 M NaOH. Batch adsorption experiments [31,32] were conducted by adding 4 g L^{-1} of the adsorbent (SMNPs) in different initial concentrations of $K_2Cr_2O_7$ solutions. These solutions were then taken in 100 ml stopper conical flasks and agitated on a thermostatic shaker (Narang Scientific) for 24 h until equilibrium was attained [33,34]. The adsorbent was then separated from the Cr(VI) solution by magnetic decantation method. Magnetic decantation method is more efficient than the centrifugation as well as filtration methods [35]. Finally, the residual concentration of Cr(VI) solutions was measured with the help of UV/visible spectrophotometer (Perkin Elmer) at a wavelength of 540 nm using the 1, 5-diphenylcarbazide (Merck) method. The adsorption capacity or the amount of metal ions adsorbed at equilibrium (q_e) per unit mass of the adsorbent is calculated by Eq. (1).

$$q_e = (C_0 - C_e) \times \frac{V}{m} \tag{1}$$

Here, C_0 and C_e are the initial and equilibrium concentrations of Cr(VI) solution (in mg L^{-1}), respectively. Further, V denotes the volume of the solution in liters and m is the mass of adsorbent in grams. Accordingly, the percentage adsorption of Cr(VI) ions is given by Eq. (2).

$$\%Ad = \frac{(C_0 - Ce)}{C_0} \times 100 \tag{2}$$

3. Results and discussion

3.1. Characterization of SMNPs adsorbent

XRD patterns of the synthesized SMNPs are shown in Fig. 1. We observe that SMNPs XRD patterns exhibit (3 1 1), (4 4 0), (5 1 1), (2 2 0), and (4 0 0) diffraction planes characteristic of the magnetite phase. One also observes that no other crystalline phase peaks could

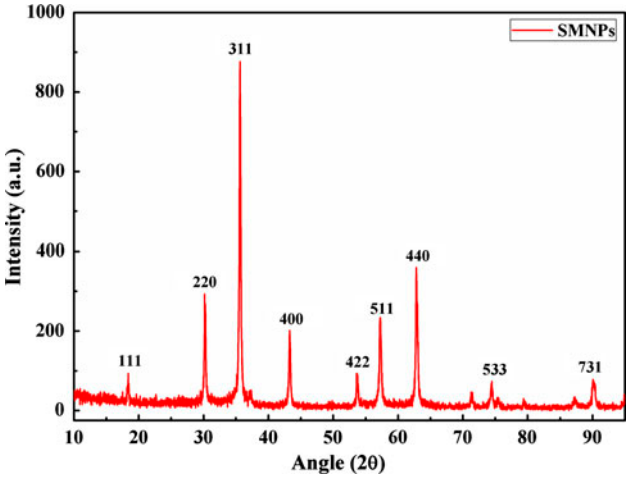

Fig. 1. XRD patterns of SMNPs sample.

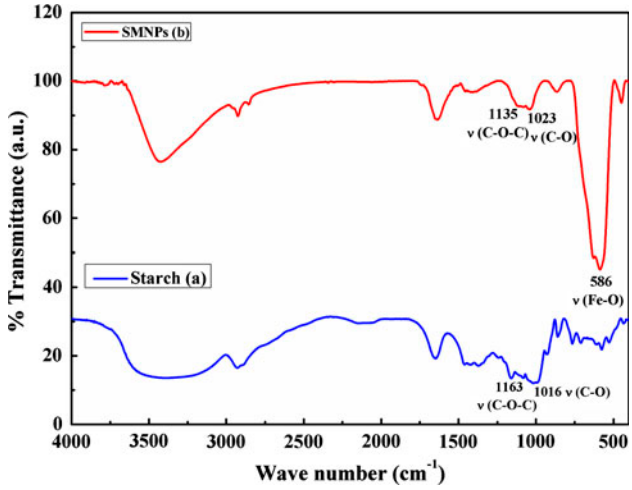

Fig. 2. Comparative FTIR plots of (a) Starch and (b) SMNPs samples to demonstrate the starch functionalization of nanoparticles.

be detected; therefore, the synthesized samples consisted only of pure magnetite phase nanoparticles. We conclude that starch functionalization does not affect the crystalline nature of the prepared samples [36]. FTIR spectra of starch and SMNPs are shown in Fig. 2(a) and (b). In Fig. 2(a), FTIR spectrum of starch shows characteristic peaks at 1,163 and 1,016 cm^{-1}. These correspond to the IR stretching frequency of glycosidic bonds (C–O–C) and C–O bonds, respectively. Compared to this, the FTIR spectrum of SMNPs displays slight shifting of the IR stretching frequencies of the glycosidic and C–O bonds at 1,135 and 1,023 cm^{-1}, respectively. In addition to these fundamental peaks of starch, we also observe another intense IR peak at 586 cm^{-1} which represents the Fe–O bond of SMNPs [37–40]. This confirms that the starch is chemisorbed on to the surface of magnetite nanoparticles. Fig. 3(a) displays a typical TEM image of SMNPs showing spherical nanoparticles. Fig. 3(b) gives the normalized particle size distribution of SMNPs obtained using the ImageJ analysis software. A large number of TEM images from different regions of the sample were used to compile the SMNPs size statistics used to prepare Fig. 3(b) [41–45].

The plot of magnetization verses magnetic field (M-H loop) at room temperature for SMNPs is shown

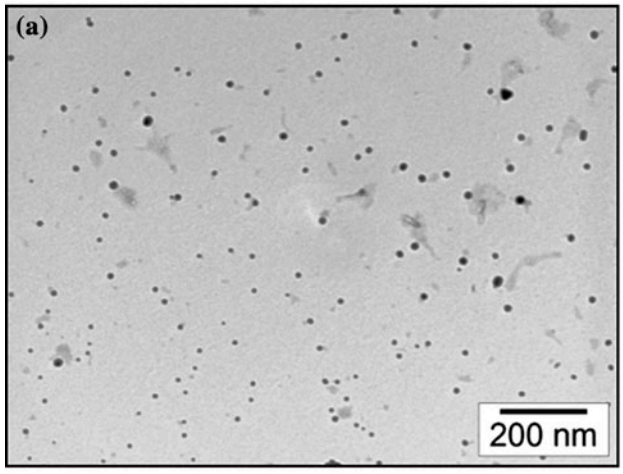

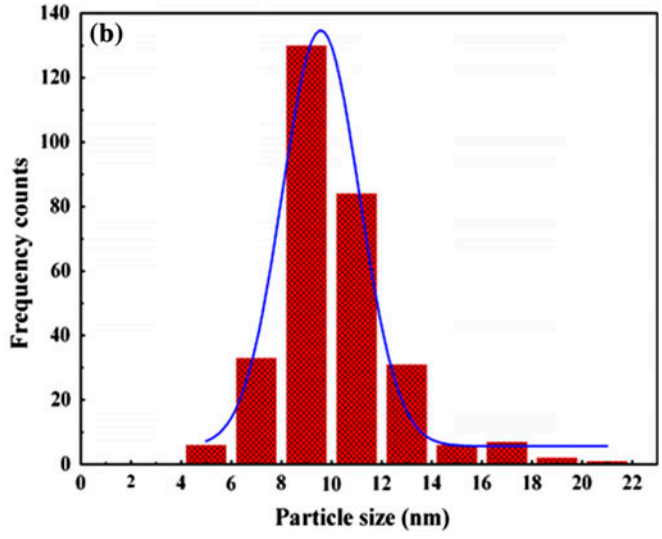

Fig. 3. (a) A typical TEM image of SMNPs sample showing spherical nanoparticles and (b) the normalized particle sizes distributions found using the TEM images from different regions the SMNPs sample.

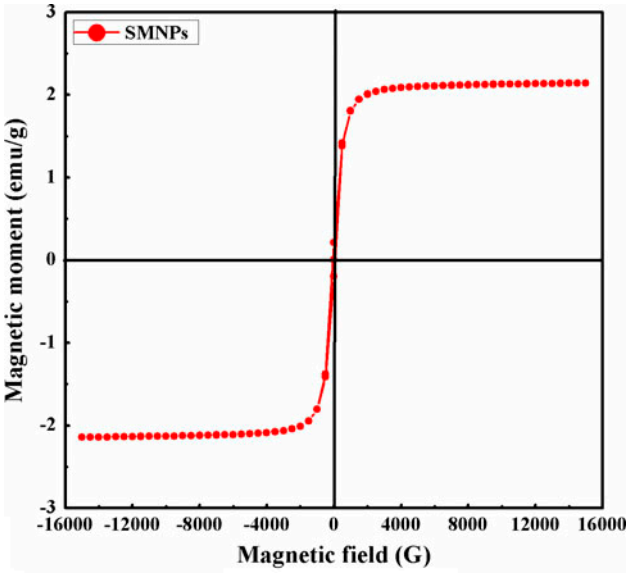

Fig. 4. Magnetic moment verses magnetic field graph of SMNPs.

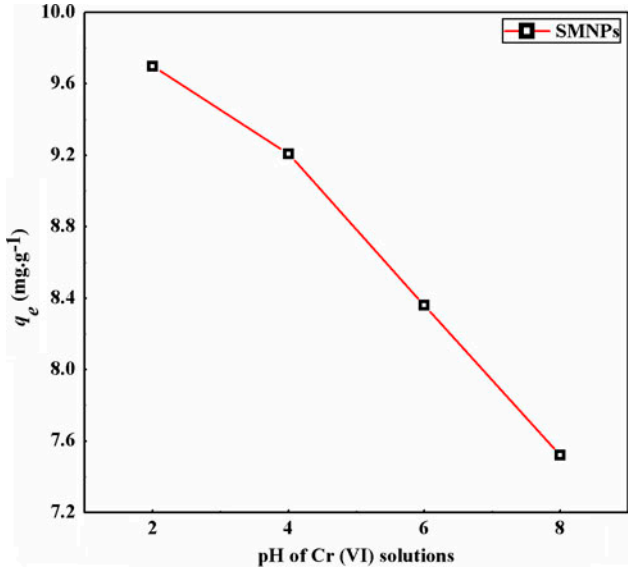

Fig. 5. Shows effect of pH on Cr(VI) ions removal by adsorbent samples through q_e (mg g^{-1}) vs. pH plots.

in Fig. 4. The magnetization curve of SMNPs was measured using vibrating sample magnetometer (Lakeshore VSM 7410). Typical superparamagnetic hysteresis characteristics were observed. In absence of external magnetic field the synthesized superparamagnetic nanoparticles do not show any magnetic property. Various magnetic measurement results of SNMPs are given in Table 1. As reported by Liu et al., the lower M_s value obtained for SMNPs may be occurring because of the decrease in the particle size and consequently large deformations on the surface of small particles [46–48].

3.2. Effect of pH on adsorption properties

Fig. 5 shows the effect of pH on the removal of Cr (VI) ions by the SMNPs from the aqueous medium. All experiments relating to effect of pH on adsorption capacity were carried out at 4 ppm initial solution concentration. At 298 K and pH 2, the adsorption capacity (q_e) is highest and it decreases with increase in pH of the Cr(VI) solution. This may be explained in the following manner. In aqueous medium, the iron oxide surface is hydroxyl functionalized [49]. Further, as mentioned earlier, starch functionalization also seems to provide access to some additional free hydroxyl functional groups of glucose units on the nanoparticle surfaces. These hydroxyl groups may react with acids or bases to be positively or negatively charged depending on whether the pH less than or greater its point of zero charge (PZC), respectively [50]. Thus, to understand better the possible mechanism of Cr(VI) adsorption, we determined the PZC of the SMNPs adsorbent (Fig. 6). The PZC for SMNPs was determined by the salt addition method and the pH_{pzc} value was found to be 6.33 [51–53]. In more acidic pH conditions (for $pH < pH_{pzc}$), there are more H^+ ions that make SMNPs surfaces positively charged. Now in acidic medium, the dominant forms of Cr(VI) ions are $HCrO_4^-$ and $HCr_2O_7^-$, while in basic medium dominant forms of Cr (VI) ions are CrO_4^{2-} and $Cr_2O_7^{2-}$ [54]. Therefore, the higher adsorption removal efficiency we observed in acidic medium may be due to electrostatic interaction

Table 1
VSM measurement results for SMNPs sample

Reaction temperature	SMNPs		
	Magnetization saturation (M_s) (emu/g)	Remnant magnetization (M_r) (emu/g)	Coercivity (H_{ci}) (gauss)
80℃	53.55	5.133	64.76

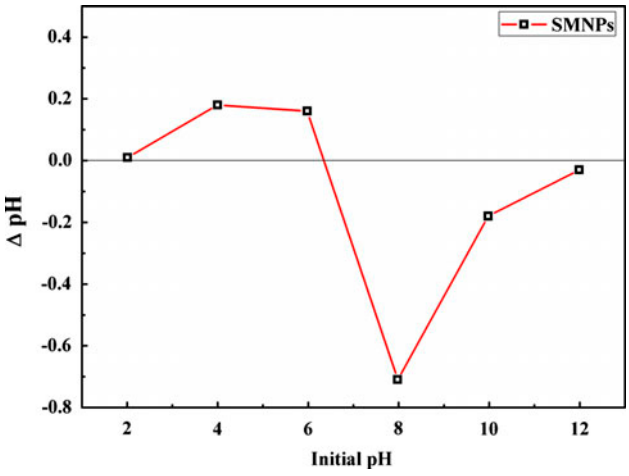

Fig. 6. ΔpH vs. initial pH plots for determination of the pH_{pzc} of SMNPs adsorbent sample. Lines joining the data points are only meant as a guide to the eye.

between the positively charged adsorbent surface and the negatively charged Cr(VI) adsorbate species. With the increase in pH, the SMNPs surfaces are less positively charged. Alternatively, in alkaline pH conditions (for $pH > pH_{pzc}$) due to the presence of more OH^- ions, SMNPs surfaces are negatively charged [55]. With the increase in pH, the removal efficiency of Cr(VI) decreased because of two reasons. Firstly, as mentioned earlier, SMNPs adsorption surfaces are negatively charged at $pH > pH_{pzc}$. Hence, there is increased electrostatic repulsion between negatively charged CrO_4^{2-} and negatively charged SMNPs surfaces. Further, at higher pH, OH^- ions compete with CrO_4^{2-} species for adsorption sites leading to decrease in removal efficiency with increase in pH.

3.3. Adsorbate concentration and adsorption isotherms

In order to investigate the adsorption capacity (q_e) of SMNPs, the initial concentration of Cr(VI) was varied from 4 to 12 ppm. All such adsorption experiments were carried out at pH 2 (the pH at which optimum adsorption occurs). Adsorption capacity (q_e) was found to increase with the initial bulk adsorbate concentration. This variation is quantified by an adsorption isotherm that depicts the typical relationship between the adsorbate on the surface of adsorbent as a function of its concentration in the solution at a particular temperature. In the present study, adsorption isotherms were evaluated at 30°C and at the optimum pH 2. These data are tested for Langmuir, Freundlich, and Temkin adsorption isotherm models. While the best model fitting to our data is obtained for the Freundlich adsorption isotherm, the data also fit well to the Langmuir isotherm. Table 2 summarizes the fit details of the experimental data to both Freundlich and Langmuir models. In contrast to the Langmuir model, the Freundlich model does not predict surface saturation and also assumes the possibility of the existence of a multi-layered structure. The Freundlich adsorption model also assumes that different adsorbent binding sites are not equal and adsorbent surface may be heterogeneous. The linearized form of the Freundlich adsorption isotherm equation [56,57] can be written in the following manner.

$$\log q_e = \log K_F + \frac{1}{n}\log C_e \tag{3}$$

Thus, the values of the Freundlich constants K_F and n are determined from the intercepts and slopes of this graph, respectively. The linear fit to $\log q_e$ vs. $\log C_e$ plots is shown in Fig. 7. The value of K_F for removal of Cr(VI) by SMNPs from aqueous solutions at 298 K and pH 2 is found to be 23.45 mg g^{-1} with n equal to 2.39 L g^{-1}. On the other hand, the maximum adsorption capacity experimentally found (when the initial Cr(VI) concentration is 12 ppm) is 26.6 mg g^{-1}. This adsorption capacity value of SMNPs is about 20–30% higher than recent reports of magnetite nanoparticles being used as adsorbents for removal of Cr(VI) from aqueous medium [58,59]. This adsorption capacity is significantly higher than the first report by Hu et al investigating magnetite nanoparticles as adsorbents (16.9 mg g^{-1} adsorption capacity) for removal of Cr (VI) from aqueous medium [60]. Further, this value for Cr(VI) removal is also better than many other

Table 2
Freundlich and Langmuir adsorption isotherms fitting parameters for Cr(VI) adsorption on to the surface of SMNPs at 303 K and at pH 2

Freundlich constant parameter			Langmuir constant parameter		
K_F (mg g^{-1})	n (L g^{-1})	R^2	Q^0 (mg g^{-1})	b (L mg^{-1})	R^2
23.45	2.397	0.999	32.69	2.91	0.9695

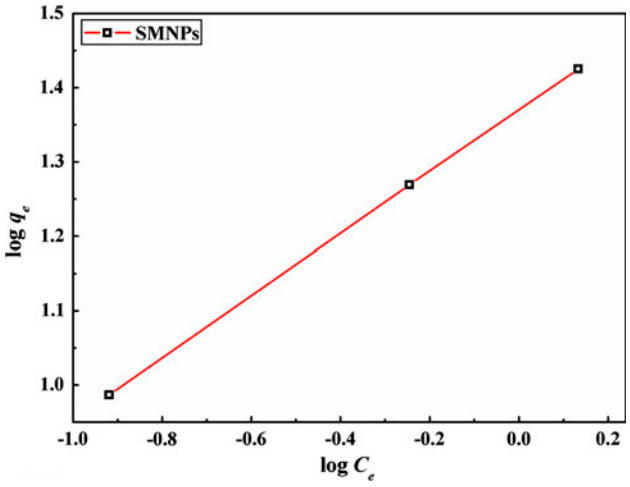

Fig. 7. Freundlich adsorption isotherm plot for removal of Cr(VI) ions by SMNPs adsorbents.

adsorbents [61–64]. Table 3 compares the adsorption capacity of various adsorbents for removal of Cr(VI) with that of the present study [65–73].

This improvement in adsorption of Cr(VI) due to starch functionalization of magnetite nanoparticles may be explained in the following way. As surmised earlier in the introduction, starch functionalization seems to provide access to some additional free hydroxyl functional groups of glucose units on the nanoparticle surfaces. These are protonated at lower pH (< pH_{ZPC}) conditions resulting in additional positive surface charge as compared to normal magnetite nanoparticles of similar size distribution. Better adsorption capacity occurs due to increase in electrostatic interaction between the positively charged SMNPs surface and the $HCrO_4^-$ anions.

3.4. Adsorption kinetic studies

Adsorption kinetics of Cr(VI) on to the surface of SMNPs was investigated at the optimum pH 2. The data obtained was fitted to both pseudo-first-order and pseudo-second-order rate expressions. However, the adsorption kinetics was found to follow pseudo-second-order kinetics much better than the first-order rate expression using Chi-square test [74]. The linear form of pseudo-second-order rate expression [75] is as given in Eq. (4).

$$\frac{t}{q_t} = \frac{1}{k_2 q_e^2} + \frac{1}{q_e} t \tag{4}$$

In above equation, k_2 denotes the rate constant for pseudo-second-order adsorption (g mg^{-1} h^{-1}) and $k_2 q_e^2$ (mg g^{-1} h^{-1}) is the initial adsorption rate and q_t is the adsorption capacity at time t. The straight line fit to plots of t/q_t vs. t (Fig. 8) confirmed that the adsorption process followed second-order kinetics. The values of adsorption capacity (q_e) and second-order rate constant (k_2) at different temperature were obtained from slope and intercept of corresponding graph, respectively. The relevant linear fit data is presented in Table 2.

3.5. Adsorption activation energy

Adsorption activation energy for the adsorption of Cr(VI) on the surface starch-functionalized magnetite nanoparticles has been calculated with the help of Arrhenius equation. The Arrhenius adsorption activation energy is given by the following expression.

Table 3
Compares the adsorption capacity of various conventional adsorbents with Starch-functionalized magnetite nanoparticles for removal of Cr(VI)

S. No.	Adsorbents	Adsorbent capacity (mg g^{-1})	References
1	Wheat bran	0.94	[43]
2	Activated alumina	1.60	[44]
3	Modified oak sawdust	1.70	[45]
4	Sawdust	3.60	[46]
5	Mixed maghemite–magnetite nanoparticles	3.60	[47]
6	Magnetite nanoparticle	11.23	[48]
7	Diatomite	11.55	[49]
8	Anatase	14.56	[50]
9	Commercial activated carbon	15.47	[51]
10	Beech sawdust	16.13	[52]
11	Maghemite	19.20	[14]
12	Magnetite nanoparticle	22.00	[37]
13	Magnetite nanoparticle	25.36	Present study
14	Starch-functionalized magnetite nanoparticles	26.60	Present study

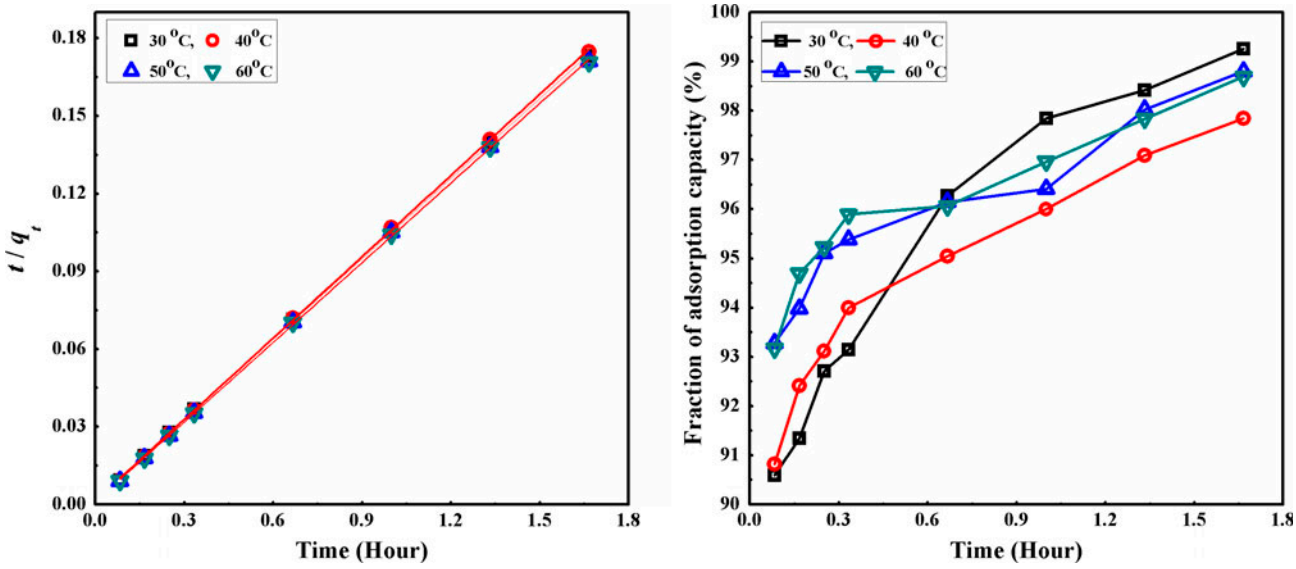

Fig. 8. The pseudo-second-order kinetics graph of SMNPs sample: (a) t/q_t vs. at time (t) at different temperatures and (b) Fraction of adsorption capacity verses time (t) at different temperatures.

$$\ln k_2 = \ln A - \frac{E_a}{RT} \quad (5)$$

Here, A is the temperature independent pre-exponential factor (g mg^{-1} h^{-1}), E_a is the adsorption activation energy (kJ mol^{-1}), R is the universal gas constant (8.314 J mol^{-1} K^{-1}), and T is the solution temperature (K). Adsorption rate constant for the adsorbate (Cr (VI)) on the surface adsorbent were calculated at number of temperatures (Table 2) from experimental data assuming pseudo-second-order rate equation. Now, these values are plotted against $1/T$ (Fig. 9).

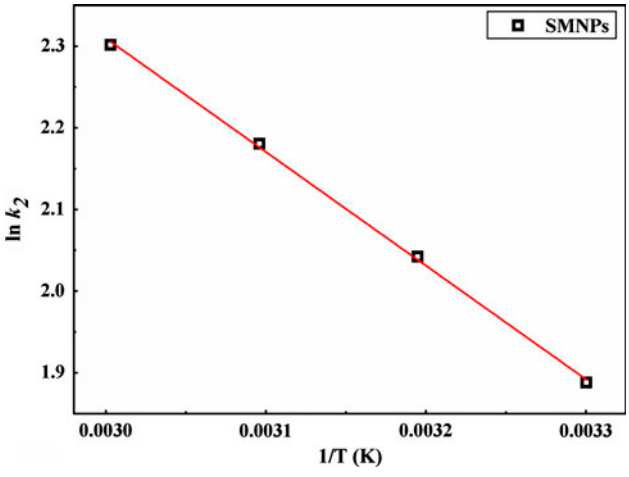

Fig. 9. ln k_2 vs. $1/T$ plots for determination of adsorption activation energy of SMNPs.

The adsorption activation energy is obtained from the slope ($-E_a/R$) of the straight line graph. The adsorption activation energy for the Cr(VI) adsorption on the surface of starch-stabilized magnetite nanoparticles is found to be 11.57 kJ mol^{-1}. Now, physisorption involves smaller activation energy values ranging from 5 to 40 kJ mol^{-1}. On other hand, chemisorptions are specific and require larger adsorption activation energy e.g. 40–800 kJ mol^{-1} due to chemical bond formation between the adsorbate and adsorbent [76–80]. Thus, the activation energy obtained in the present investigation indicates that Cr (VI) was physically adsorbed on the surface of SMNPs.

3.6 Recovery and recycle evaluation

Very low activation energy of Cr(VI) adsorption on to SMNPs meant that the adsorption could be reversible and therefore, the technologically attractive possibility of adsorbent regeneration and reuse was investigated. The first step in this process involves adsorbent regeneration and then the recovery of the component adsorbed on the adsorbent surface [81–83]. From adsorption experiments at different pH, we know that Cr(VI) adsorption on SMNPs decreases with increase in pH. Therefore, desorption of Cr(VI) from SMNPs was carried out in basic medium. This was done by shaking the Cr(VI)-loaded adsorbent in 0.1 M NaOH solution for 24 h at 298 K. After the completion of this desorption treatment, SMNPs were washed thoroughly with distilled water until no more

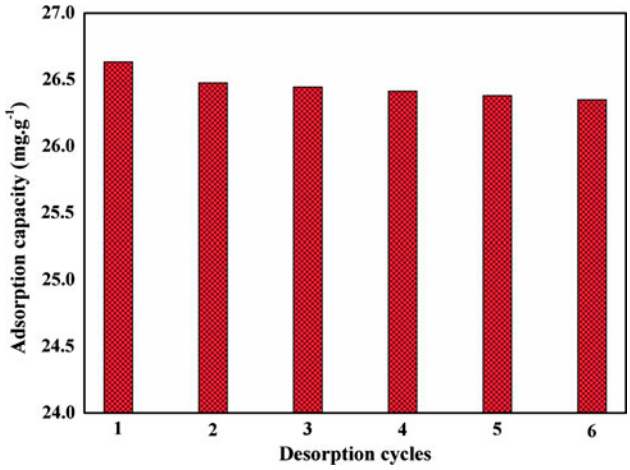

Fig. 10. Adsorption capacity (q_e) vs. desorption cycle plot for recovery and recycle evaluation of SMNPs for Cr(VI) removal.

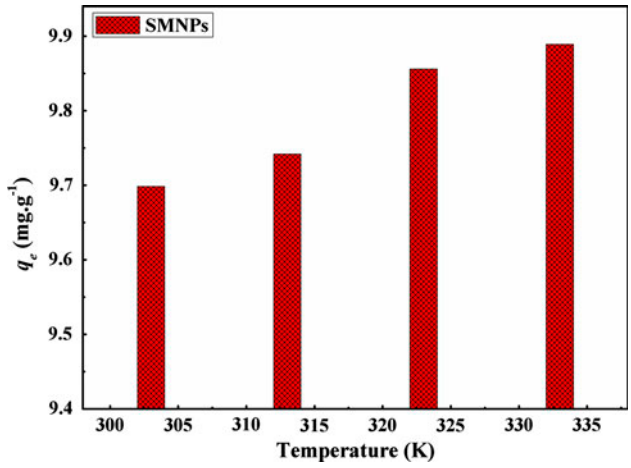

Fig. 11. Graph of q_e variation with adsorption temperature.

Cr(VI) could be detected in the washings and the filtrate also became neutral. The recovered SMNPs were subjected to the adsorption protocol as given in Section 2.2. The adsorbent was recovered and reused for six consecutive cycles. Fig. 10 shows variation of adsorption capacity vs. such desorption cycles. Very little (%) decrease in adsorption capacity of SMNPs, for Cr(VI), was observed even after six consecutive cycles. Please note that the amount of reused adsorbent was kept constant in repeat cycles although more than 90% of the SMNPs could be recovered after washing. The amount of SMNPs/reused adsorbent was kept constant in all desorption cycles by carrying out several parallel adsorption-desorption experiments. Adsorbent loss in each cycle was compensated from such parallel experiments.

3.7. Effect of temperature on adsorption properties

Fig. 11 displays the effect of temperature on Cr(VI) ions' removal from aqueous solutions by SMNPs. Adsorption capacity for Cr(VI) removal increases as the temperature is changed from 303 to 333 K. That higher temperature leads to increased adsorption capacity indicates endothermic adsorption of Cr(VI) ions on SMNPs surface. An increase in Cr(VI) removal with the temperature may be due to increase in the number of adsorption surface active sites at higher temperature by the breakage of some bonds near adsorption surface active site.

3.8. Adsorption thermodynamics studies

The dependency of the equilibrium constant (K) vs. $1/T$ for the binding of chromium ions on the adsorbent was analyzed in terms of van't Hoff plots. The thermodynamic parameters of adsorption process such as change in standard free energy (ΔG°), enthalpy (ΔH°), and entropy (ΔS°) are calculated [84] at different temperatures 303, 313, and 323 K using Eqs. (6)–(8).

$$\Delta G^\circ = -RT \ln K \tag{6}$$

$$\Delta H^\circ = R\left(\frac{T_2 T_1}{T_2 - T_1}\right) - \ln\left(\frac{K_1}{K_2}\right) \tag{7}$$

Table 4
Fit parameters obtained by linear fitting the kinetic experimental data (for removal of Cr(VI) by SMNPs adsorbents) to the pseudo-second-order rate expression (Eq. (4)) at different temperatures

	Removal of Cr(VI) by SMNPs			
Temperature (K)	q_e (mg g^{-1})	k_2 (g mg^{-1} h^{-1})	R^2	X
303	9.6927	5.6338	0.999	0.001891
313	9.56022	7.7053	0.999	0.058804
323	9.7446	8.8494	0.999	0.03566

Table 5
Thermodynamic parameters of adsorption of Cr(VI) on to SMNPs at different temperatures. Values presented in this table were obtained from experiments done with initial 4 ppm Cr(VI) aqueous solution concentration and at the optimum pH 2

Temperature (K)	ΔG° (kJ mol^{-1})	ΔH° (kJ mol^{-1})	ΔS° (J mol^{-1} K^{-1})
303	−8.74458	78.84	289.085
313	−9.44969	84.05	306.26
323	−11.34915	89.42	323.98

$$\Delta S^\circ = \frac{\Delta H^\circ - \Delta G^\circ}{T} \quad (8)$$

Here, K is the equilibrium constant, R is ideal gas constant (8.314 J mol^{-1} K^{-1}), and T is the absolute temperature. The details of these thermodynamic parameters are given in Table 5. The negative value of ΔG° and positive value of ΔH° indicate that the reaction is spontaneous and endothermic in nature [85]. As mentioned in sub-Section 3.6, the endothermic process might be attributed to some bond breaking with increasing temperature resulting in increased number of active sites on the adsorbent sites. The positive entropy change (ΔS°) (Table 5) indicates that the degree of randomness increases during the adsorption process.

4. Conclusions

Superparamagnetic starch-functionalized pure phase magnetite nanoparticles (SMNPs) synthesized by a co-precipitation method were used as nanoadsorbents for removal of hexavalent chromium from aqueous medium. The removal efficiency of Cr(VI) was found to be highly pH dependent with optimum adsorption occurring at pH 2. The isotherm data for SMNPs adsorbents best fitted the Freundlich adsorption isotherm model, suggesting a physical adsorption mechanism. From the experimental data at different temperatures, the adsorption process was found to have a low energy of activation characteristic of physisorption. Owing to this low adsorption activation energy, the adsorbent demonstrated excellent regeneration and reuse capacity. The Cr(VI) adsorption process on to SMNPs followed pseudo-second-order kinetics. From the thermodynamic studies, we conclude that the adsorption process was endothermic in nature with increase in randomness at the adsorbent–adsorbate interface.

Acknowledgment

We acknowledge Department of Anatomy, Institute of Medical Sciences (BHU) for their help in TEM imaging and Sophisticated Analytical Instrument Facility, Indian Institute of Technology Madras for the VSM characterisation. One of authors (P.N. Singh) is thankful to University Grant Commission, Government of India, for providing the financial assistantship in the form of a senior research fellowship (SRF).

References

[1] J.J. Testa, M.A. Grela, M.I. Litter, Heterogeneous photocatalytic reduction of chromium(VI) over TiO_2 particles in the presence of oxalate: Involvement of Cr (V) species, Environ. Sci. Technol. 38 (2004) 1589–1594.
[2] N. Shevchenko, V. Zaitsev, A. Walcarius, Bifunctionalized mesoporous silicas for Cr(VI) reduction and concomitant Cr(III) immobilization, Environ. Sci. Technol. 42 (2008) 6922–6928.
[3] V.K. Gupta, D. Pathania, S. Agarwal, S. Sharma, Removal of Cr(VI) onto *Ficus carica* biosorbent from water, Environ. Sci. Pollut. Res. 20 (2013) 2632–2644.
[4] V.K. Gupta, M. Gupta, S. Sharma, Process development for the removal of lead and chromium from aqueous solutions using red mud—An aluminium industry waste, Water Res. 35 (2001) 1125–1134.
[5] Y.G. Zhao, H.Y. Shen, S.D. Pan, M.Q. Hu, Q.H. Xia, Preparation and characterization of amino-functionalized nano-Fe_3O_4 magnetic polymer adsorbents for removal of chromium(VI) ions, J. Mater. Sci. 45 (2010) 5291–5301.
[6] V.K. Gupta, I. Ali, T.A. Saleh, M.N. Siddiqui, S. Agarwal, Chromium removal from water by activated carbon developed from waste rubber tires, Environ. Sci. Pollut. Res. 20 (2013) 1261–1268.
[7] V.K. Gupta, A.K. Shrivastava, N. Jain, Biosorption of chromium(VI) from aqueous solutions by green algae spirogyra species, Water Res. 35 (2001) 4079–4085.
[8] V.K. Gupta, S. Agarwal, T.A. Saleh, Chromium removal by combining the magnetic properties of iron oxide with adsorption properties of carbon nanotubes, Water Res. 45 (2011) 2207–2212.
[9] V.K. Gupta, A. Rastogi, Sorption and desorption studies of chromium(VI) from nonviable cyanobacterium *Nostoc muscorum* biomass, J. Hazard. Mater. 154 (2008) 347–354.
[10] M. Shi, Z. Li, Y. Yuan, T. Yue, J. Wang, R. Li, J. Chen, In situ oxidized magnetite membranes from 316L porous stainless steel via a two-stage sintering process for hexavalent chromium [Cr(VI)] removal from aqueous solutions, Chem. Eng. J. 265 (2015) 84–92.
[11] V.K. Gupta, A. Rastogi, Biosorption of hexavalent chromium by raw and acid-treated green alga *Oedogonium hatei* from aqueous solutions, J. Hazard. Mater. 163 (2009) 396–402.

[12] V.K. Gupta, D. Pathania, S. Sharma, S. Agarwal, P. Singh, Remediation of noxious chromium(VI) utilizing acrylic acid grafted lignocellulosic adsorbent, J. Mol. Liq. 177 (2013) 343–352.
[13] V.K. Gupta, A. Rastogi, A. Nayak, Adsorption studies on the removal of hexavalent chromium from aqueous solution using a low cost fertilizer industry waste material, J. Colloid Interface Sci. 342 (2010) 135–141.
[14] S.K. Srivastava, V.K. Gupta, D. Mohan, Removal of lead and chromium by activated slag—A blast-furnace waste, J. Environ. Eng. 123 (1997) 461–468.
[15] S.K. Srivastava, V.K. Gupta, D. Mohan, Kinetic parameters for the removal of lead and chromium from wastewater using activated carbon developed from fertilizer waste material, Environ. Model. Assess. 1 (1996) 281–290.
[16] V.K. Gupta, I. Ali, Removal of lead and chromium from wastewater using bagasse fly ash-a sugar industry waste, J. Colloid Interface Sci. 271 (2004) 321–328.
[17] A. Mittal, D. Kaur, A. Malviya, J. Mittal, V.K. Gupta, Adsorption studies on the removal of coloring agent phenol red from wastewater using waste materials as adsorbents, J. Colloid Interface Sci. 337 (2009) 345–354.
[18] V.K. Gupta, A. Nayak, Cadmium removal and recovery from aqueous solutions by novel adsorbents prepared from orange peel and Fe_2O_3 nanoparticles, Chem. Eng. J. 180 (2012) 81–90.
[19] P.N. Singh, D. Tiwary, I. Sinha, Improved removal of Cr(VI) by starch functionalized iron oxide nanoparticles, J. Environ. Chem. Eng. 2 (2014) 2252–2258.
[20] V.K. Singh, P.N. Tiwari, Removal and recovery of chromium(VI) from industrial waste water, J. Chem. Technol. Biotechnol. 69 (1997) 376–382.
[21] N.K. Lazaridis, D.D. Asouhidou, Kinetics of sorptive removal of chromium(VI) from aqueous solutions by calcined Mg–Al–CO3 hydrotalcite, Water Res. 37 (2003) 2875–2882.
[22] W. Tang, Z. Peng, L. Li, T. Yue, J. Wang, Z. Li, R. Li, J. Chen, V.L. Colvin, W.W. Yu, Porous stainless steel supported magnetite crystalline membranes for hexavalent chromium removal from aqueous solutions, J. Membr. Sci. 392–393 (2012) 150–156.
[23] Y. Zhang, N. Kohler, M. Zhang, Surface modification of superparamagnetic magnetite nanoparticles and their intracellular uptake, Biomaterials 23 (2002) 1553–1561.
[24] C.T. Yavuz, J.T. Mayo, W.W. Yu, A. Prakash, J.C. Falkner, S. Yean, L. Cong, H.J. Shipley, A. Kan, M. Tomson, D. Natelson, V.L. Colvin, Low-field magnetic separation of monodisperse Fe_3O_4 nanocrystals, Science 314 (2006) 964–967.
[25] X.Q. Xu, H. Shen, J.R. Xu, J. Xu, X.J. Li, X.M. Xiong, Core-shell structure and magnetic properties of magnetite magnetic fluids stabilized with dextran, Appl. Surf. Sci. 252 (2005) 494–500.
[26] E. Khor, L.Y. Lim, Implantable applications of chitin and chitosan, Biomaterials 24 (2003) 2339–2349.
[27] T.T. Dung, T.M. Danh, L.T.M. Hoa, D.M. Chien, N.H. Duc, Structural and magnetic properties of starch-coated magnetite nanoparticles, J. Exp. Nanosci. 4 (2009) 259–267.
[28] A.K. Gupta, M. Gupta, Synthesis and surface engineering of iron oxide nanoparticles for biomedical applications, Biomaterials 26 (2005) 3995–4021.
[29] S. Alibeigi, M.R. Vaezi, Phase transformation of iron oxide nanoparticles by varying the molar ratio of Fe^{2+}: Fe^{3+}, Chem. Eng. Technol. 31 (2008) 1591–1596.
[30] H. Kazemzadeh, A. Ataie, Synthesis of magnetite nano-particles by reverse, Int. J. Mod. Phys. 5 (2012) 160–167.
[31] H. Aono, H. Hirazawa, T. Naohara, T. Maehara, H. Kikkawa, Y. Watanabe, Synthesis of fine magnetite powder using reverse coprecipitation method and its heating properties by applying AC magnetic field, Mater. Res. Bull. 40 (2005) 1126–1135.
[32] V.K. Gupta, I. Ali, T.A. Saleh, A. Nayak, S. Agarwal, Chemical treatment technologies for waste-water recycling—An overview, RSC Adv. 2 (2012) 6380–6388.
[33] S. Yean, L. Cong, C.T. Yavuz, J.T. Mayo, W.W. Yu, A.T. Kan, V.L. Colvin, M.B. Tomson, Effect of magnetite particle size on adsorption and desorption of arsenite and arsenate, J. Mater. Res. 20 (2005) 3255–3264.
[34] J. Hu, G. Chen, I.M.C. Lo, Removal and recovery of Cr(VI) from wastewater by maghemite nanoparticles, Water Res. 39 (2005) 4528–4536.
[35] P. Wang, I.M.C. Lo, Synthesis of mesoporous magnetic γ-Fe2O3 and its application to Cr(VI) removal from contaminated water, Water Res. 43 (2009) 3727–3734.
[36] A.K. Bajpai, S. Likhitkar, Investigation of magnetically enhanced swelling behaviour of superparamagnetic starch nanoparticles, Bull. Mater. Sci. 36 (2013) 15–24.
[37] A.K. Bajpai, J. Shrivastava, In vitro enzymatic degradation kinetics of polymeric blends of cross-linked starch and carboxymethyl cellulose, Polym. Int. 54 (2005) 1524–1536.
[38] D.K. Kim, M. Mikhaylova, F.H. Wang, J. Kehr, B. Bjelke, Y. Zhang, T. Tsakalakos, M. Muhammed, Starch-coated superparamagnetic nanoparticles as MR contrast agents, Chem. Mater. 15 (2003) 4343–4351.
[39] Y.F. Shen, J. Tang, Z.H. Nie, Y.D. Wang, Y. Ren, L. Zuo, Preparation and application of magnetic Fe_3O_4 nanoparticles for wastewater purification, Sep. Purif. Technol. 68 (2009) 312–319.
[40] T. Dey, C.J.O. Connor, Preparation and application of magnetic Fe_3O_4 nanoparticles for wastewater purification, Sep. Purif. Technol. 2 (2005) 13–16.
[41] S.K. Janardhanan, I. Ramasamy, B.U. Nair, Synthesis of iron oxide nanoparticles using chitosan and starch templates, Transition Met. Chem. 33 (2008) 127–131.
[42] A. Taubert, G. Wegner, Formation of uniform and monodisperse zincite crystals in the presence of soluble starch, J. Mater. Chem. 12 (2002) 805–807.
[43] Q. Liang, D. Zhao, T. Qian, K. Freeland, Y. Feng, Effects of stabilizers and water chemistry on arsenate sorption by polysaccharide-stabilized magnetite nanoparticles, Ind. Eng. Chem. Res. 51 (2012) 2407–2418.
[44] J.S. Jiang, Z.F. Gan, Y. Yang, B. Du, M. Qian, P. Zhang, A novel magnetic fluid based on starch-coated magnetite nanoparticles functionalized with homing peptide, J. Nanopart. Res. 11 (2009) 1321–1330.
[45] Y.M. Soshnikova, S.G. Roman, N.A. Chebotareva, O.I. Baum, M.V. Obrezkova, R.B. Gillis, S.E. Harding, E.N. Sobol, V.V. Lunin, Starch-modified magnetite nanoparticles for impregnation into cartilage, J. Nanopart. Res. 15 (2013) 2092–2102.

[46] Z.L. Liu, Y.J. Liu, K.L. Yao, Z.H. Ding, J. Tao, X. Wang, Synthesis and magnetic properties of Fe_3O_4 nanoparticles, J. Mater. Synth. Process. 10 (2002) 83–87.
[47] V.S. Zaitsev, D.S. Filimonov, I.A. Presnyakov, R.J. Gambino, B. Chu, Physical and chemical properties of magnetite and magnetite-polymer nanoparticles and their colloidal dispersions, J. Colloid. Interface Sci. 212 (1999) 49–57.
[48] D.H. Chen, M.H. Liao, Preparation and characterization of YADH-bound magnetic nanoparticles, J. Mol. Catal. B: Enzym. 16 (2002) 283–291.
[49] A.M.G.C. Dias, A. Hussain, A.S. Marcos, A.C.A. Roque, A biotechnological perspective on the application of iron oxide magnetic colloids modified with polysaccharides, Biotechnol. Adv. 29 (2011) 142–155.
[50] J.C. Bacri, R. Perzynski, D. Salin, Ionic ferrofluids: A crossing of chemistry and physics, J. Magn. Magn. Mater. 85 (1990) 27–32.
[51] T. Mahmood, M.T. Saddique, A. Naeem, P. Westerhoff, S. Mustafa, A. Alum, Comparison of different methods for the point of zero charge determination of NiO, Ind. Eng. Chem. Res. 50 (2011) 10017–10023.
[52] M. Kosmulski, pH-dependent surface charging and points of zero charge, J. Colloid Interface Sci. 298 (2006) 730–741.
[53] Y.C. Chang, D.H. Chen, Preparation and adsorption properties of monodisperse chitosan-bound Fe_3O_4 magnetic nanoparticles for removal of Cu(II) ions, J. Colloid Interface Sci. 283 (2005) 446–451.
[54] M.P. Candela, J.M.M. Martinez, R.T. Macia, Chromium(VI) removal with activated carbons, Water Res. 29 (1995) 2174–2180.
[55] S.R. Chowdhury, E.K. Yanful, A.R. Pratt, Chemical states in XPS and Raman analysis during removal of Cr(VI) from contaminated water by mixed maghemite–magnetite nanoparticles, J. Hazard. Mater. 235–236 (2012) 246–256.
[56] Y. Li, B. Gao, T. Wu, D. Sun, X. Li, B. Wang, F. Lu, Hexavalent chromium removal from aqueous solution by adsorption on aluminum magnesium mixed hydroxide, Water Res. 43 (2009) 3067–3075.
[57] A. Mittal, J. Mittal, A. Malviya, D. Kaur, V.K. Gupta, Decoloration treatment of a hazardous triarylmethane dye, Light Green SF (Yellowish) by waste material adsorbents, J. Colloid Interface Sci. 342 (2010) 518–527.
[58] T.M. Do, Y.J. Suh, Removal of aqueous Cr(VI) using magnetite nanoparticles synthesized from a low grade iron ore, Par. Aerosol Res. 9 (2013) 221–230.
[59] P. Yuan, D. Liu, M. Fan, D. Yang, R. Zhu, F. Ge, J.X. Zhu, H. He, Removal of hexavalent chromium [Cr (VI)] from aqueous solutions by the diatomite-supported/unsupported magnetite nanoparticles, J. Hazard. Mater. 173 (2010) 614–621.
[60] J. Hu, I.M.C. Lo, G. Chen, Removal of Cr(VI) by magnetite nanoparticle, Water Sci. Technol. 50 (2004) 139–146.
[61] G.H. Pino, L.M.S. de Mesquita, M.L. Torem, Biosorption of heavy metals by powder of green coconut shell, Sep. Sci. Technol. 41 (2006) 3141–3153.
[62] S.S. Banerjee, M.V. Joshi, R.V. Jayaram, Removal of Cr(VI) and Hg(II) from aqueous solutions using fly ash and impregnated fly ash, Sep. Sci. Technol. 39 (2004) 1611–1629.
[63] N.R. Bishnoi, M. Bajaj, N. Sharma, A. Gupta, Adsorption of Cr(VI) on activated rice husk carbon and activated alumina, Bioresour. Technol. 91 (2004) 305–307.
[64] M. Nameni, M.R. Alavi Moghadam, M. Arami, Adsorption of hexavalent chromium from aqueous solutions by wheat bran, Int. J. Environ. Sci. Technol. 5 (2008) 161–168.
[65] N.R. Bishnoi, M. Bajaj, N. Sharma, A. Gupta, Adsorption of Cr(VI) on activated rice husk carbon and activated alumina, Bioresour. Technol. 91 (2004) 305–307.
[66] M.E. Argun, S. Dursun, C. Ozdemir, M. Karatas, Heavy metal adsorption by modified oak sawdust: Thermodynamics and kinetics, J. Hazard. Mater. 141 (2006) 77–85.
[67] S.S. Baral, S.N. Das, P. Rath, Hexavalent chromium removal from aqueous solution by adsorption on treated sawdust, Biochem. Eng. J. 31 (2006) 216–222.
[68] S.R. Chowdhury, E.K. Yanful, A.R. Pratt, Chemical states in XPS and Raman analysis during removal of Cr(VI) from contaminated water by mixed maghemite–magnetite nanoparticles, J. Hazard. Mater. 235–236 (2012) 246–256.
[69] J. Hu, I.M.C. Lo, G. Chen, Removal of Cr(VI) by magnetite nanoparticle, Water Sci. Technol. 50 (2004) 139–146.
[70] T.N.D. Dantas, A.A.D. Neto, M.C.P. Moura, Removal of chromium from aqueous solutions by diatomite treated with microemulsion, Water Res. 35 (2001) 2219–2224.
[71] C.H. Weng, J.H. Wang, C.P. Huang, Adsorption of cr(vi) onto tio from dilute aqueous solutions, Water Sci. Technol. 35 (1997) 55–62.
[72] B. Sandhya, A.K. Tonnin, Cr(VI) removal from synthetic wastewater using coconut shell charcoal and commercial activated carbon modified with oxidizing agents and/or chitosan, Chemosphere 54 (2004) 951–967.
[73] F.N. Acar, E. Malkoc, The removal of chromium(VI) from aqueous solutions by *Fagus orientalis* L., Bioresour. Technol. 94 (2004) 13–15.
[74] H.K. Boparai, M. Joseph, D.M. O'Carroll, Kinetics and thermodynamics of cadmium ion removal by adsorption onto nano zerovalent iron particles, J. Hazard. Mater. 186 (2011) 458–465.
[75] A. Mittal, J. Mittal, A. Malviya, V.K. Gupta, Adsorptive removal of hazardous anionic dye ''Congo red'' from wastewater using waste materials and recovery by desorption, J. Colloid Interface Sci. 340 (2009) 16–26.
[76] D. Zhang, Y. Ma, H. Feng, Y. Hao, Adsorption of Cr(VI) from aqueous solution using carbon-microsilica composite adsorbent, J. Chil. Chem. Soc. 57 (2012) 964–968.
[77] M. Doğan, M. Alkan, Adsorption kinetics of methyl violet onto perlite, Chemosphere 50 (2003) 517–528.
[78] E. Malkoc, Y. Nuhoglu, Potential of tea factory waste for chromium(VI) removal from aqueous solutions: Thermodynamic and kinetic studies, Sep. Purif. Technol. 54 (2007) 291–298.

[79] W.B. Zhang, M. Deng, C.X. Sun, S.B. Wang, Ultrasound-enhanced adsorption of chromium(VI) on Fe_3O_4 magnetic particles, Ind. Eng. Chem. Res. 53 (2014) 333–339.
[80] Y.S. Ho, G. McKay, Sorption of dye from aqueous solution by peat, Chem. Eng. J. 70 (1998) 115–124.
[81] J. Hu, G. Chen, I.M.C. Lo, Removal and recovery of Cr(VI) from wastewater by maghemite nanoparticles, Water Res. 39 (2005) 4528–4536.
[82] M.R. Lasheen, I.Y. El-Sherif, D.Y. Sabry, S.T. El-Wakeel, M.F. El-Shahat, Removal and recovery of Cr(VI) by magnetite nanoparticles, Desalin. Water Treat. 52 (2014) 6464–6473.
[83] J. Hu, I.M.C. Lo, G. Chen, Fast removal and recovery of Cr(VI) using surface-modified jacobsite ($MnFe_2O_4$) nanoparticles, Langmuir 21 (2005) 11173–11179.
[84] A. Mittal, J. Mittal, A. Malviya, V.K. Gupta, Removal and recovery of Chrysoidine Y from aqueous solutions by waste materials, J. Colloid Interface Sci. 344 (2010) 497–507.
[85] T. Fan, Y. Liu, B. Feng, G. Zeng, C. Yang, M. Zhou, H. Zhou, Z. Tan, X. Wang, Biosorption of cadmium (II), zinc(II) and lead(II) by *Penicillium simplicissimum*: Isotherms, kinetics and thermodynamics, J. Hazard. Mater. 160 (2008) 655–661.